

Article

Effect of Synthesis Time on Synthesis and Photoluminescence Properties of ZnO Nanorods

Cheng-Fu Yang^{1,2}, Ching-Shan Wang³, Fang-Hsing Wang^{3,*}, Han-Wen Liu³ and Julia Micova^{4,*}

¹ Department of Chemical and Materials Engineering, National University of Kaohsiung, Kaohsiung, Taiwan; cfyang@nuk.edu.tw

² Department of Aeronautical Engineering, Chaoyang University of Technology, Taichung 413, Taiwan

³ Graduate Institute of Optoelectronic Engineering, National Chung Hsing University, Taichung 402, Taiwan; ching.shan73@msa.hinet.net (Wang); fansen@dragon.nchu.edu.tw (Wang), hwliu@dragon.nchu.edu.tw (Liu)

⁴ Institute of Chemistry, Slovak Academy of Sciences, SK-845 38 Bratislava, Slovakia; Julia.Micova@savba.sk

* Correspondence: fansen@dragon.nchu.edu.tw (Wang); Julia.Micova@savba.sk (J. Micova)

Received: Feb 14, 2022; Accepted: Mar 14, 2022; Published: Mar 30, 2022

Abstract: With the hydrothermal method, the p-type silicon <100> wafer was used as the substrate to synthesize ZnO nanorods in different synthesis times. To prepare the ZnO seed layer on the p-type silicon <100> wafer, a prepared ZnO gel was deposited as the seed layer using the spin coating method. A 0.2 M solution of zinc acetate dihydrate ($Zn(CH_3COO)_2 \cdot 2H_2O$) and hexamethylenetetramine ($(CH_2)_6N_4$) were used as the source materials at a synthesis temperature of 90 °C. The synthesis time was changed from 10 to 60 min as the synthesis parameter. X-ray diffraction patterns, scanning electron microscopy, and a focused ion beam system were used to analyze and compare the crystal characteristics and the heights and widths of synthesized ZnO nanorods. We found that the crystal characteristics, the heights and widths, and the photoluminescence properties of synthesized ZnO nanorods were dependent on the synthesis time.

Keywords: Hydrothermal method, P-type silicon <100> wafer, Synthesis time, ZnO nanorods

1. Introduction

In the past, many different synthesis methods and process technologies had been investigated to fabricate ZnO-based nanomaterials with different morphologies and various crystal shapes [1–3]. For example, Zhang et al. used a capping-molecule-assisted hydrothermal process to investigate ZnO microcrystals [4]. They found that the synthesized formations of dumbbell-like, disk-like, and flower-like shapes of ZnO microcrystals depended on the used capping molecules. Wang et al. also used the hydrothermal method to synthesize ZnO microcrystals [5]. They found that controlling the pH of the solution, the reaction time, and the concentration of the precursor affected the flower-like rod aggregation, hexagonal pyramid-like rod, and microrod appearances of ZnO nanomaterials. The hydrothermal method is the most economical, simple, and commonly used method to synthesize ZnO nanostructures.

ZnO-based nanomaterials are applied in various optoelectronic devices and, thus, it is important to develop methods to synthesize ZnO. In this study, we used the hydrothermal method to synthesize ZnO nanorods and nanoflower arrays using ZnO seed layers on different substrates. In general, ZnO nanorods are synthesized on planar substrates perpendicular to the substrate. When ZnO nanorods are used as sensors for different signals, the first sites for contact and reaction are at the top surfaces of the nanorods. When ZnO nanorods are grown in a structure of radiating needles, they form ZnO nanoflowers. When ZnO nanoflowers are used as gas or optical sensors, they have a greater area for contact and reaction sites and then enhance the reaction sensitivity and the response speed.

This study used the hydrothermal method to synthesize ZnO nanorods and investigated the effect of synthesis time on the properties of synthesized ZnO nanorods. We used a precursor solution with a concentration of 0.2 M, which was composed of zinc acetate dihydrate ($Zn(CH_3COO)_2 \cdot 2H_2O$) and hexamethylenetetramine, and a series of experiments were carried out to synthesize ZnO nanorods with a synthesis temperature of 90 °C. During the experiments, the synthesis time was varied from 10 to 60 min, but the synthesis temperature and the precursor solution concentration were kept constant. The microstructure and physical properties of these synthesized ZnO nanorods strongly depend on the synthesis time of the hydrothermal method.

2. Materials and Methods

First, ZnO seed layers were deposited on the substrate. Its method was as follows: 2-aminoethanol (monoethanolamine) (C_2H_7NO), zinc acetate dihydrate ($Zn(CH_3COO)_2 \cdot 2H_2O$), and ethylene glycol monomethyl ether ($CH_3OCH_2CH_2OH$) were used to prepare a solution of 0.75 M Zn^+ ions ($Zn(CH_3COO)_2 \cdot 2H_2O$). The prepared solution was heated at $60 \text{ }^\circ\text{C}$ and stirred for 2 h to form a uniform solution. The solution was then left in the air for 48 h to obtain a transparent ZnO sol solution. To prepare the ZnO seed layer, first, the ZnO gel was applied to fully cover the surface of a p-type Si $\langle 100 \rangle$ wafer. The spin coating method, at a speed of 2,000 RPM for 30 s, was used to spread the gel. The ZnO gel-coated template was then baked at $300 \text{ }^\circ\text{C}$ for 10 min to dry and harden the coating film and to volatilize and remove the organic solvent. The spin coating and baking processes were repeated six times, after which a ZnO thin layer was obtained. A synthesis temperature of $90 \text{ }^\circ\text{C}$, synthesis times of 10, 20, 30, and 60 min, and a 0.2 M solution of zinc acetate dihydrate ($Zn(CH_3COO)_2 \cdot 2H_2O$) and hexamethylenetetramine ($(CH_2)_6N_4$) were used to synthesize the ZnO nanorods. After the ZnO nanorods were synthesized, the crystalline phases were analyzed using an X-ray diffractometer (XRD). The surface morphologies of the ZnO seed layer and synthesized ZnO nanorods were observed by using a field emission scanning electron microscope (FESEM). The height (or length), diameter, morphology, and aspect ratio of the prepared nanorods were also estimated. The prepared patterned ZnO seed layer and synthesized ZnO nanorods were cut using a focused ion beam (FIB) system to observe their cross-sectional morphologies. A Horiba Jobin Yvon iHR550 fluorescence spectrophotometer was used to measure the photoluminescence (PL) emission properties of synthesized ZnO nanorods at room temperature and in the wavelength range of 350–650 nm. The excitation light source was the single wavelength laser at a wavelength of 325 nm.

3. Results and Discussion

The surface morphology and the cross-sectional image of the ZnO seed layer on the p-type Si $\langle 100 \rangle$ wafer are shown in Fig. 1. We used ZnO gel (i.e., as the precursor) and the spin coating method to prepare the ZnO seed layer. Although the deposited film was annealed at $300 \text{ }^\circ\text{C}$, the porous state of each particle was distinct at the surface, as shown in Fig. 1(a). The particles were about 30 nm in size, which matched the results obtained using the Debye–Scherrer's equation and the diffraction peak of the (002) plane from Fig. 2. Fig. 1(b) shows that the thickness of the ZnO seed layer was about 198 nm, which suggests that the thickness of each coating was approximately 33 nm.

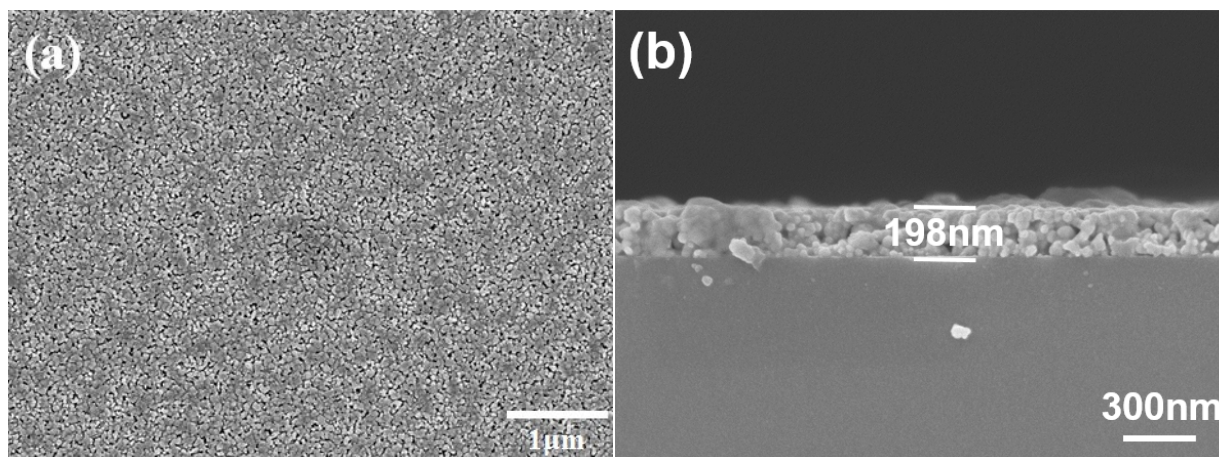
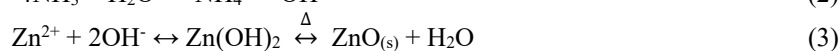
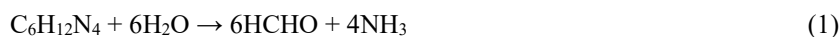


Fig. 1 (a) Surface morphology and (b) cross-sectional image of ZnO-seed layer.

The chemical reactions involved in the fabrication of ZnO nanorods were divided into metal oxide hydrolysis and dehydration reactions. The chemical reactions are listed below [6,7].



From the chemical reaction equilibrium, we determine the direction of these chemical equilibrium reactions by controlling the concentrations of the reactants, the synthesis temperature, and the synthesis time. In general, the concentrations of the reactants determine the density of one-dimension ZnO nanorods, while the synthesis temperature and synthesis time affect the morphology, including the diameter, height, and aspect ratio of ZnO nanorods.

In this study, the synthesis time is the parameter to investigate the properties of ZnO nanorods. The XRD patterns of ZnO nanorods as a function of synthesis time are shown in Fig. 2. We used XRD patterns to identify the type of material as well as its phase and crystalline properties. For ZnO crystal, there is an apparent diffraction peak located at the 2θ value of 34.7° , corresponding to the (002) plane. The diffraction peaks located at the 2θ values of 31.9° , 36.48° , 47.64° and 56.78° corresponds to the (100), (101), (102) and (110) planes, respectively. Fig. 2 shows that the diffraction patterns of ZnO nanorods synthesized with different synthesis time. It was found that there were three diffraction peaks in each pattern. The peak intensity of the (002) plane increased with the synthesis time, which suggests that the crystal quality of ZnO nanorods in the (002) plane improved with time. Fig. 2 also shows that the peak intensities of the (100) and (101) planes decreased with time. There was no (102) and (110) diffraction peaks in the XRD patterns. These results indicate that the prepared ZnO nanorods had a *c*-axis preferred orientation, and the synthesis rate of the peaks along the (002) plane is more sensitive to synthesis time than the (100) and (101) planes with increasing synthesis time.

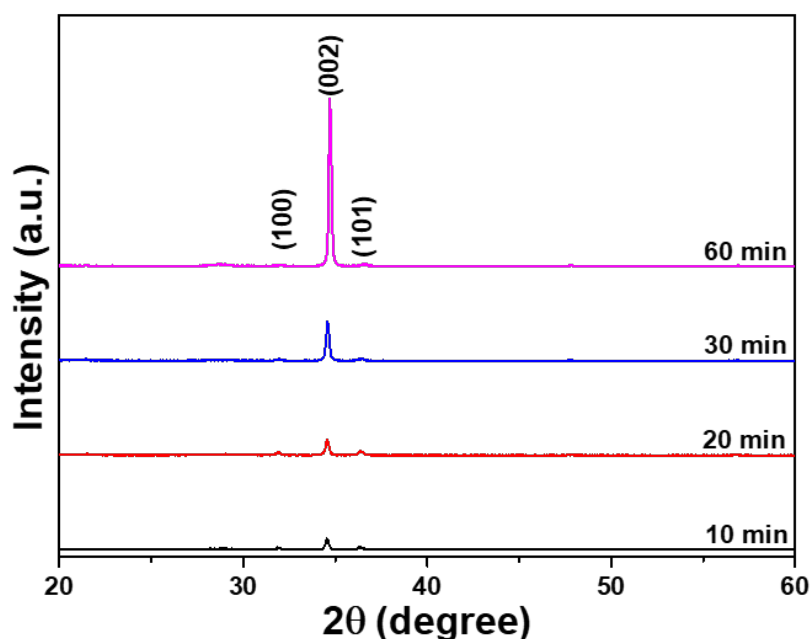


Fig. 2. XRD patterns of ZnO nanorods as a function of synthesis time.

The top and cross-sectional morphologies of ZnO nanorods with various synthesis times are shown in Figs. 3 and 4, respectively. From these figures, the height (i.e., length) and diameter of ZnO nanorods were determined, and then the aspect ratio (the height divided by the diameter) was calculated using the measured values to analyze the relationship between the axial and radial growth of ZnO nanorods. The height and the diameter of 10 ZnO nanorods were measured to find their average values for synthesis times of 10, 20, 30, and 60 min. When the thickness of the ZnO seed layer was determined to be 200 nm, the average heights of ZnO nanorods were 42, 130, 335, and 1300 nm, and their average diameters were 54, 71, 88, and 112 nm, respectively. Correspondingly, the calculated aspect ratios of ZnO nanorods were 0.78, 1.83, 3.80, and 11.6 when the synthesis time was 10, 20, 30, and 60 min, respectively. From the results, the height, diameter, and aspect ratio of ZnO nanorods were closely related to the synthesis time. From the results, ZnO nanorods were observed even when the synthesis time was only 10 min. As the synthesis time increased, both the height and the diameter of ZnO nanorods increased significantly, and thus the aspect ratio also increased significantly. However, the density of ZnO nanorods in a unit area decreased with synthesis time. Because the ZnO nanorods push against each other, they grow perpendicular to the substrate and, therefore, the diffraction intensities of the (100) and (101) planes gradually become weaker. Therefore, the synthesis time of 60 min is optimal for the synthesis of ZnO nanorods with high length, high aspect ratio, and well-defined hexagonal prism shape.

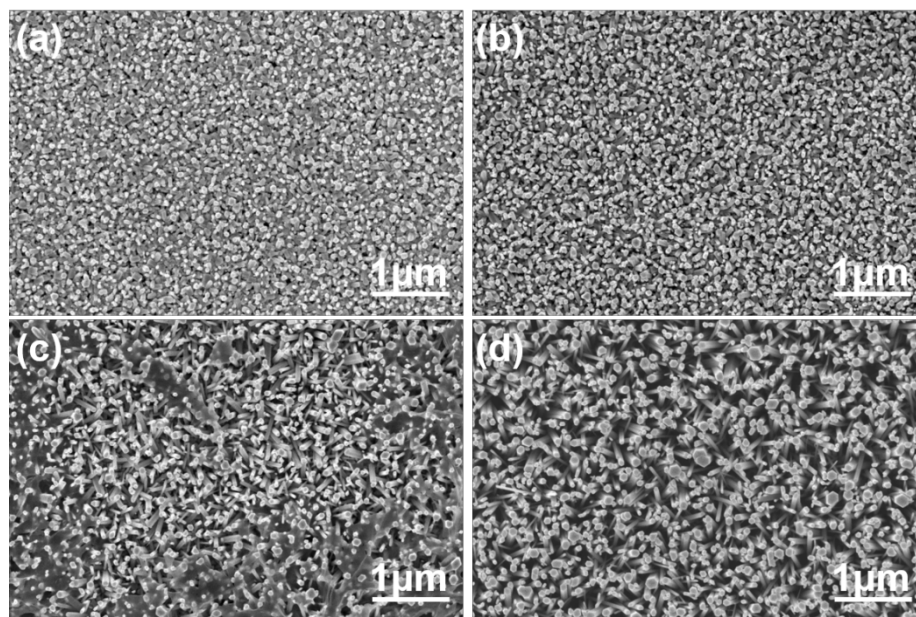


Fig. 3. SEM images of the surface morphologies of ZnO nanorods as a function of synthesis time: (a) 10 min, (b) 20 min, (c) 30 min, and (d) 60 min.

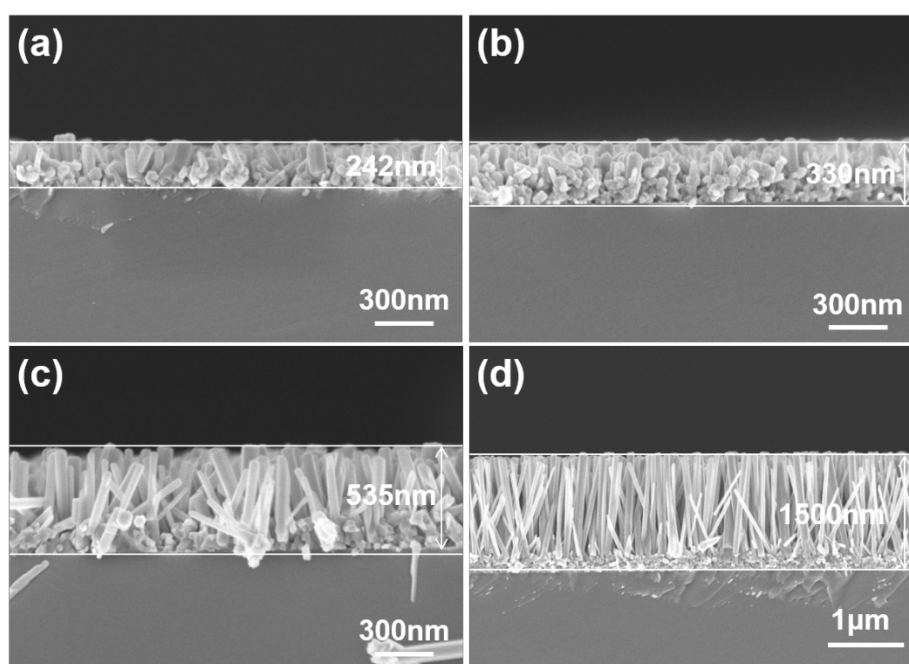


Fig. 4. Cross-sectional morphologies of ZnO nanorods as a function of synthesis time, (a) 10 min, (b) 20 min, (c) 30 min, and (d) 60 min.

To calculate the density (i.e., quantity) of ZnO nanorods per unit area, the surface area was divided into squares with an area of $1 \mu\text{m}^2$ as shown in Fig. 5. We randomly sampled 8 squares, calculated the density of ZnO nanorods in each square, and determined the average value. The densities of ZnO nanorods were 107, 94, 72, and $65 \mu\text{m}^{-2}$ when the synthesis time was 10, 20, 30, and 60 min, respectively. The measured heights and diameters, as well as the calculated densities, of the ZnO nanorods, were used to determine the total surface area (S, nm^2), the total volume (V, nm^3), and the S/V ratio. The results shown in Table 1 are as a function of synthesis time. As the synthesis time increased from 10 to 60 min, the total surface area increased from 1.01×10^6 to $3.04 \times 10^7 \text{ nm}^2$, the total volume increased from 1.03×10^7 to $8.32 \times 10^8 \text{ nm}^3$ and the S/V ratio decreased from 9.79×10^{-2} to 3.65×10^{-2} . These results indicate that it is possible to change the height, diameter, and aspect ratio of ZnO nanorods by controlling the synthesis time.

The main reason for the increases in total surface area and total volume was that the height and diameter of ZnO nanorods increased with synthesis time, while the density of ZnO nanorods decreased with synthesis time. The results in Table 1 reveal that the growth rate of ZnO nanorods in the vertical-axis direction (i.e., perpendicular to the substrate) was higher than that in the radial-axis direction, even though the density per unit area decreased with time. ZnO-based materials have a stable crystal plane group, including nonpolar surface groups of $\{10\bar{1}0\}$ and $\{2\bar{1}\bar{1}0\}$, and a polar surface group of $\{0001\}$. In ZnO-based materials, the polar surface is caused by negatively charged oxygen ions and positively charged zinc ions, which form a vertical dipole interaction torque on the *c*-axis plane [8]. Therefore, the growth rate in the vertical-axis direction is higher than that in the radial-axis direction, which causes the ZnO nanorods to have a *c*-axis preferred orientation with a high aspect ratio at a long synthesis time.

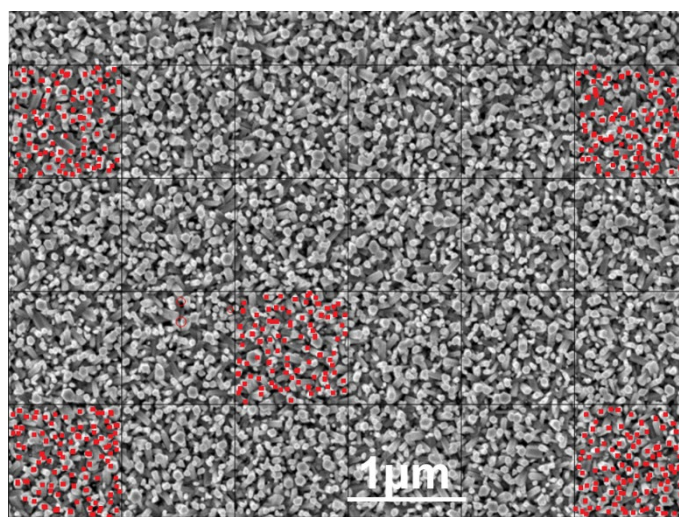


Fig. 5. Surface morphology was used to calculate the density of ZnO nanorods.

When the hydrothermal method is used to synthesize ZnO nanomaterials, the polar $\{0001\}$ plane has a better activity response than the nonpolar $\{10\bar{1}0\}$ and $\{2\bar{1}\bar{1}0\}$ planes. Therefore, the ZnO materials have a *c*-axis preferred orientation when forming one-dimensional nanomaterials, such as nanorods or nanowires. Two factors cause an increase in the diameter and a decrease in the density of ZnO nanorods. First, during the synthesis process, two adjacent nanorods may combine to form one nanorod, which causes the diameter of the nanorod to increase and the density to decrease. Second, because the growth rate of the nanorods is inconsistent, those with a fast growth rate will remove elements they need, which can cause nanorods that have a slow growth rate to synthesize slower or to stop synthesizing. This causes the density of the nanorods to decrease and the diameter to increase.

Table 1. Density, total surface area (*S*), total volume (*V*), and *S/V* ratio of ZnO nanorods as a function of synthesis time.

Synthesis time (min)	10	20	30	60
Density (quantity per μm^2)	107	94	72	65
Total surface area (<i>S</i> , nm^2)	1.01×10^6	3.10×10^6	7.10×10^6	3.04×10^6
Total volume (<i>V</i> , nm^3)	1.03×10^7	4.84×10^7	1.47×10^8	8.32×10^8
<i>S/V</i> ratio	9.79×10^{-2}	6.40×10^{-2}	4.84×10^{-2}	3.65×10^{-2}

Fig. 6 shows the PL intensities of ZnO nanorods with various synthesis time. It was found that the PL emission strongly depended on the synthesis time. Table 2 shows the emission intensity values of UV (ultraviolet) light (I_{UV}), green light (I_G), and the I_G/I_{UV} ratio of ZnO nanorods for different synthesis times. As the synthesis time increased from 10 to 60 min, the intensity of the I_{UV} value increased from 224 to 742 (a.u.), while the I_G value decreased from 150 to 60.7 and the I_G/I_{UV} ratio decreased from 0.670 to 0.082. It is well accepted that the crystal quality of ZnO nanorods is closely associated with the intensity of the UV and near-band-edge emission, and that the emission intensity in the range of 420–575 nm is closely related to defects, such as interstitial oxygen and antisite defects [9]. It was found that the broad emission intensity of the ZnO seed layer at 420–575 nm was higher than the intensity for the ZnO nanorods at all synthesis times. This result suggested that the ZnO seed layer contained many different defects and had poor crystal quality. The decreased I_G and I_G/I_{UV} values of nanorods with synthesis time indicated that the defects in the ZnO nanorods decreased and the crystal quality of ZnO nanorods was improved with the increasing synthesis time. This result is consistent with the XRD analysis shown in Fig. 2.

Li et al. found that an increase in the intensity of UV light was related to the S/V ratio [10]. When the S/V ratio was high, the I_{UV} value was high and the I_G value was low. However, the present research showed a different trend. The I_{UV} of ZnO nanorods was positively related to the total surface area and the total volume and was negatively related to the S/V ratio. The increase in the S/V ratio was caused by an increase in the total surface area, which provided more area to absorb the excited light and emit the emission light. Therefore, we believe that the large total surface area enhanced the I_{UV} of ZnO nanorods. Besides, Vanheusden et al. reported that the near-band-edge emission intensity was closely related to the crystal quality of the prepared ZnO samples [9]. From Fig. 6 and Tab. 2, the I_G/I_{UV} ratio exhibited a decreasing trend with the increasing synthesis time. Thus, the total surface area and the crystal quality of ZnO nanorods are important factors that affect the PL properties.

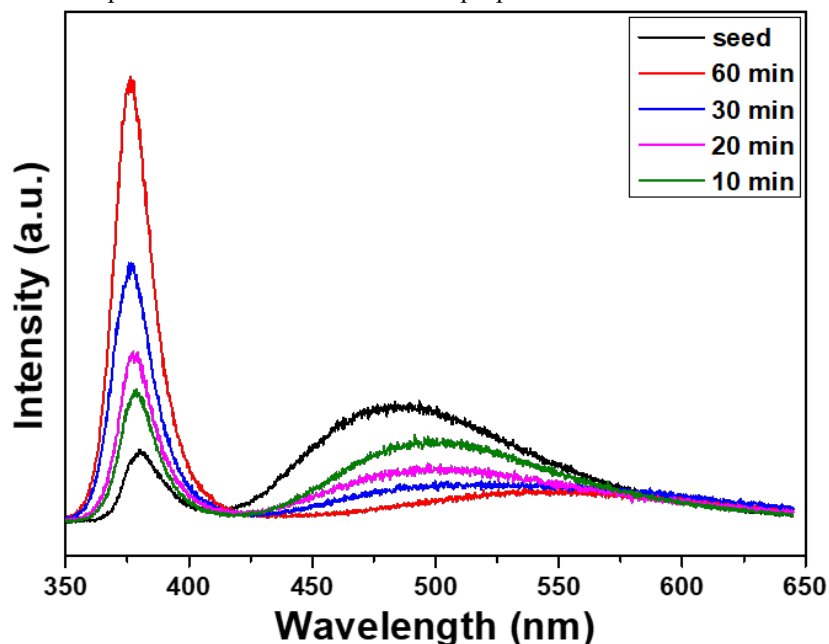


Fig. 6. PL emission spectra of ZnO nanorods as a function of synthesis time.

Table 2. I_{UV} values, I_G values, and the I_G/I_{UV} ratio of ZnO nanorods as a function of synthesis time.

Synthesis time (min)	I_{UV}	I_G	I_G/I_{UV}
10	224	150	0.670
20	287	103	0.359
30	434	74.4	0.171
60	742	60.7	0.082

4. Conclusions

ZnO nanorods have been synthesized by using hydrothermal method with different synthesis times on seeded p-type silicon <100> substrate. The thickness of the ZnO seed layer was about 198 nm and its surface particles were about 30 nm in size. The prepared ZnO nanorods had a c-axis preferred orientation when the synthesis time increased, and the synthesis rate along the peak of the (002) plane was more sensitive to the synthesis time compared with the peaks of the (100) and (101) planes. For the synthesis times of 10, 20, 30, and 60, the average heights of ZnO nanorods were 42, 130, 335, and 1300 nm, and the average diameters of ZnO nanorods were 54, 71, 88, and 112 nm, respectively. As the synthesis time increased from 10 to 60 min, the total surface area increased from 1.01×10^6 to 3.04×10^7 nm², the total volume increased from 1.03×10^7 to 8.32×10^8 nm³, and the S/V ratio decreased from 9.79×10^{-2} to 3.65×10^{-2} . These results demonstrate that it is possible to manipulate the height, diameter, and aspect ratio of ZnO nanorods by controlling the synthesis time. The PL analysis showed that the I_G/I_{UV} ratio decreased from 0.670 to 0.082 as the synthesis time increased from 10 to 60 min. These results demonstrate that one can control the morphology and crystal quality of ZnO nanorods by adjusting the synthesis time during the hydrothermal process.

Author Contributions: Conceptualization, C.F. Yang, F.H. Wang and Julia Micova; methodology, C.F. Yang, C.S. Wang, F.H. Wang, H.W. Liu and Julia Micova; validation, C.F. Yang, C.S. Wang, F.H. Wang and Julia Micova; formal analysis, C.F. Yang, F.H. Wang and Julia Micova; investigation, C.F. Yang, C.S. Wang, F.H. Wang and Julia Micova; data curation, C.F. Yang, C.S. Wang and F.H. Wang; writing—original draft preparation, C.F. Yang, F.H. Wang and Julia Micova; writing—review and editing, C.F. Yang, F.H. Wang and Julia Micova. All authors have read and agreed to the published version of the manuscript.

Acknowledgments: This work was supported by projects under Nos. MOST 110-2622-E-390-002 and MOST 110-2221-E-390-020.

Conflicts of Interest: The authors declare no conflict of interest.

References

1. Chen, Y.C.; Cheng, H.Y.; Yang, C.F.; Hsieh, Y.T. Investigate the Optimal Parameters in Hydrothermal Method for the Synthesis of ZnO Nanorods. *J. Nanomaterials*, **2014**, *2014*, 430164.
2. Wei, Y.F.; Chung, W.Y.; Yang, C.F.; Shen, J.R.; Chen, C.C. Using Different Ions in Hydrothermal Method to Enhance the Photoluminescence Properties of Synthesis ZnO-Based Nanowires. *Electronics* **2019**, *8*, 446.
3. Zheng, W.J. Tzou, W.C. Shen, J.R.; Yang, C.F.; Chen, C.C. Effect of the Concentration of Eu^{3+} Ions on Crystalline and Optical Properties of ZnO Nanowires. *Sens. Mater.* **2019**, *31*, 447–455.
4. Zhang, H.; Yang, D.; Li, D.S.; Ma, X.; Li, S.; Que, D. Controllable Growth of ZnO Microcrystals by a Capping-Molecule-Assisted Hydrothermal Process. *Cryst Growth Des.* **2005**, *5*, 547–550.
5. Wang, H.; Xie, J.; Yan, K.; Duan, M. Growth Mechanism of Different Morphologies of ZnO Crystals Prepared by Hydrothermal Method, *Journal of Materials Science and Technology. J. Mater. Sci. Technol.* **2011**, *27*, 153–158.
6. Ahsanulhaq, Q.; Umar, A.; Hahn, Y.B. Growth of aligned ZnO nanorods and nanopencils on ZnO/Si in aqueous solution: growth mechanism and structural and optical properties, *Nanotechnology* **2007**, *18*, 115603.
7. Wei, Y.F.; Chung, W.Y.; Yang, C.F.; Hsu, W.F.; Chen, C.C. Effect of Deposition Parameters on the Hydrothermal Method to Synthesize ZnO-Based Nanowires. *Sens. Mater.* **2019**, *31*, 3619–3628.
8. Li, Q.W.; Bian, J.M.; Sun, J.C.; Wang, J.W.; Luo, Y.M.; Sun, K.T.; Yu, D.Q. Controllable growth of well-aligned ZnO nanorod arrays by low-temperature wet chemical bath deposition method. *Appl Sur Sci.* **2010**, *256*, 1698–1702.
9. Vanheusden, K.; Seager, C.H.; Warren, W.L.; Tallant, D.R.; Voigt, J.A. Correlation between photoluminescence and oxygen vacancies in ZnO phosphors. *Appl Phys Lett.* **1996**, *68*, 403.
10. Ahsanulhaq, Q.; Umar, A.; Hahn, Y.B. Growth of aligned ZnO nanorods and nanopencils on ZnO/Si in aqueous solution: growth mechanism and structural and optical properties. *Nanotechnology*, **2007**, *18*, 115603.

Publisher's Note: IIKII stays neutral with regard to jurisdictional claims in published maps and institutional affiliations.

Copyright: © 2021 The Author(s). Published with license by IIKII, Singapore. This is an Open Access article distributed under the terms of the [Creative Commons Attribution License](https://creativecommons.org/licenses/by/4.0/) (CC BY), which permits unrestricted use, distribution, and reproduction in any medium, provided the original author and source are credited.